Geochimica et Cosmochimica Acta Vol. 52, pp. 395–403

0016-7037/88/$3.00 + .00

Viscosities of melts in the Na_2O-FeO-Fe_2O_3-SiO_2 system and factors controlling relative viscosities of fully polymerized silicate melts

DONALD B. DINGWELL* and DAVID VIRGO
Geophysical Laboratory, Carnegie Institution of Washington, 2801 Upton Street NW, Washington, D.C., 20008, U.S.A.

(*Received May* 12, 1987; *accepted in revised form November* 13, 1987)

Abstract—The viscosity-temperature relationships of nine melts in the Na_2O-FeO-Fe_2O_3-SiO_2 system (in equilibrium with air) have been measured in the temperature range of 1450–800°C, using the concentric cylinder method. ^{57}Fe Mössbauer spectra were obtained on quenched samples and show that all melts with ≥20 mole% ferrite component contain ≥95% Fe as tetrahedrally-coordinated ferric ions.

The compositions investigated lie along the SiO_2-$NaFeO_2$ and $Na_2Si_4O_9$-$Na_6Fe_4O_9$ joins. The viscosities of melts decrease strongly with decreasing silicate content along these joins. In contrast, the temperature dependence of viscosity does not vary significantly along these joins.

Comparison with equivalent melt compositions (related by the trivalent cation exchange operators $AlFe_{-1}$, BFe_{-1} and $GaFe_{-1}$) in the Na_2O-Al_2O_3-SiO_2, Na_2O-B_2O_3-SiO_2 and Na_2O-Ga_2O_3-SiO_2 systems, shows that viscosities decrease in the order aluminosilicate > ferrosilicate, (galliosilicate ?) > borosilicate.

The electronegativities of the trivalent cations are inversely correlated with the relative viscosities of melts in these systems. Similarly, the electronegativities of network-stabilizing cations are inversely correlated with melt viscosity for alkali and alkaline-earth aluminosilicate melt systems. The variation in the viscosity of tectosilicate melts is correlated with estimated average T-O-T bond angles, and exothermic heats of solution of quench glasses. Structural controls of viscosity discussed are tetrahedral ordering and relative bond strengths.

The acmite component in natural, peralkaline, silicic volcanics will not contribute directly to high melt viscosities for these lavas.

INTRODUCTION

VISCOSITY IS PERHAPS the single most important physical property of magmas (and lavas) (WILLIAMS and MCBIRNEY, 1979; FISHER and SCHMINKE, 1984). For relatively dry, crystal-poor, peralkaline lavas such as those of the Kenya rift zone (BAILEY and MACDONALD, 1987) the determination of lava viscosity during eruptions is largely a question of estimating 1) the temperature of eruption, and 2) the temperature-viscosity relationship of the erupted silicate melts whose compositions are probably very similar to the compositions of the glassy peralkaline rocks.

One of the most diagnostic chemical expressions of peralkalinity in the Kenyan comendites, trachytes and pantellerites is the presence of CIPW-normative acmite. Estimation of the eruptive viscosities of these lavas is, therefore, hindered by the lack of data for the viscosity-temperature relationships in the system Na_2O-FeO-Fe_2O_3-SiO_2, particularly for the acmite component. In fact, as noted by BOTTINGA and WEILL (1972), there is a paucity of viscosity data for highly oxidized iron-bearing silicate melts.

A comparison of the viscosity-temperature relationships of ferric iron- and aluminum-bearing melts may provide further insight into the relationship between melt viscosity and melt structure because (like aluminum in the Na_2O-Al_2O_3-SiO_2 system) ferric iron appears to be in tetrahedral coordination in melts in the Na_2O-FeO-Fe_2O_3-SiO_2 system that are equilibrated with air (FOX *et al.*, 1982; HENDERSON *et al.*, 1984; MYSEN *et al.*, 1980; VIRGO *et al.*, 1983) but (unlike aluminum in the Na_2-Al_2O_3-SiO_2 system) may not exhibit a random distribution of ferrite and silicate tetrahedra (MYSEN *et al.*, 1985a; VIRGO and MYSEN, 1985). Thus a comparison of melt viscosities in the Na_2O-Fe_2O_3-SiO_2 and Na_2O-Al_2O_3-SiO_2 systems might contribute to a better understanding of the relationship between viscosity and ordering of tetrahedrally-coordinated cations in these melts.

The system Na_2O-FeO-Fe_2O_3-SiO_2 was selected for an investigation of the viscosity-temperature relationships of iron-bearing silicate melts for the following additional reasons. Firstly, phase equilibria had been determined in air for the compositional region of this study (BOWEN *et al.*, 1930) ensuring that the superliquidus viscosities of the compositions were experimentally accessible. Secondly, a direct comparison of the viscosities of aluminum- and ferric iron-bearing silicate melts was possible by using existing data for the viscosity-temperature relationships of the equivalent aluminum-bearing melts in the Na_2O-Al_2O_3-SiO_2 system (RIEBLING, 1966; DINGWELL, unpublished). In addition, comparisons can be made with limited melt viscosity data for the Na_2O-B_2O_3-SiO_2 and Na_2O-Ga_2O_3-SiO_2 systems. Thirdly, previous studies of the redox state of iron in melts in the Na_2O-SiO_2-Fe-O system (VIRGO *et al.*, 1983) indicated that these melts, when equilibrated with air, would be extremely oxidized and thus the effect of ferrous iron could be minimized.

EXPERIMENTAL METHOD

Starting compositions

The compositions of melts investigated in this study are plotted in the ternary system Na_2O-Fe_2O_3-SiO_2 along the SiO_2-$NaFeO_2$ and $Na_2Si_4O_9$-$Na_6Fe_4O_9$ joins (Fig. 1). The viscosity-temperature relationships were determined for melts with 12.5, 25 and 50 mole percent $NaFeO_2$ (denoted SFN6, Fe-albite and acmite, respectively) on the

* *Present address:* Bayerishes Geoinstitut, Universität Bayreuth, Postfach 10 12 51, 8580 Bayreuth, FRG.

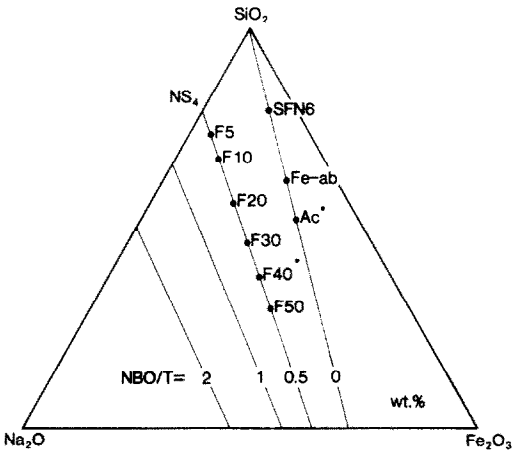

FIG. 1. The compositions of melts investigated in this study plotted in the Na_2O-Fe_2O_3-SiO_2 system. Diagram in wt.%. Asterisks refer to compositions whose oxidation state-viscosity relationships have been investigated (see text for discussion of oxidation states).

SiO_2-$NaFeO_2$ join, and for melts containing 5, 10, 20, 30, 40 and 50 mole percent $Na_6Fe_4O_9$ (denoted NS4F5, NS4F10, NS4F20, NS4F30, NS4F40 and NS4F50) on the $Na_2Si_4O_9$-$Na_6Fe_4O_9$ join.

The starting materials for viscosity determinations were glasses prepared from mixtures of reagent-grade Na_2CO_3 and Fe_2O_3, and purified quartz sand. Batches of carbonate and oxides equivalent to be decarbonated weight of 70 g were ground under alcohol in an agate mortar for 2 hours and then melted into a 25 cc thin-walled platinum crucible at 1400°C for 2 hours. These batches were poured and broken from the flexible platinum crucible and the quenched glasses were melted into a thick-walled viscometry crucible at 1450°C and stirred with a viscometry spindle for 30 min. The viscometry crucible and spindle are described below.

Viscometry

Viscosities were measured in air, in the temperature range of 1450–800°C, using the concentric cylinder method. The design and operation of the viscometer used in this study have been described by DINGWELL (1986). The samples were contained in a cylindrical $Pt_{80}Rh_{20}$ crucible (5.1 cm in height, 2.56 cm inner diameter, 0.1 cm wall thickness) in a SiC-heated vertical tube furnace. The temperatures were monitored during viscometry runs with a Pt-$Pt_{90}Rh_{10}$ thermocouple (shielded in Pt tubing) calibrated against the melting point of Au and were checked periodically with a second, shielded Pt-$Pt_{90}Rh_{10}$ thermocouple immersed in the melt sample. The accuracy of temperature determinations is taken as ±2°C.

The viscosities were determined with a Brookfield RVTD viscometer head. This viscometer head drives a spindle at a range of constant angular velocities (0.5 to 100 rpm) and digitally records the torque exerted on the spindle by the sample. Two $Pt_{80}Rh_{20}$ spindles were used in this study. Both spindles have the cross-section of a cylinder with 45° conical ends and 0.24 cm diameter stems to reduce end-effects. The low viscosity spindle has a 1.44 cm diameter and a 3.32 cm length and the high viscosity spindle has a 0.32 cm diameter and a 4.2 cm length. The viscometer head and spindles were calibrated for viscosity determinations using NBS SRM 711 standard lead-silica glass for which the temperature-viscosity relationship is accurately known. The precision of determinations involving separate occupations of the temperature set-point and separate immersions of the spindles is ±3% (2σ). The accuracy of determinations is taken as the sum of uncertainties from standard and sample determinations at ±6% (2σ). For each sample, viscosity determinations were initiated at the highest temperature and then made at successively lower temperatures. Thermal equilibrium was monitored with a chart recording of the sample viscosity during the decreasing temperature steps. One hour was sufficient for equilibration of the sample over each 50–100°C temperature decrease. At the termination of each viscometry run a high temperature viscosity measurement was redetermined to check for instrumental drift during the run. No drift was observed for any of these samples.

Torque measurements were made over a range of angular velocities for each sample. In all cases, the viscosities obtained were independent of angular velocity. At each temperature step, a Pt wire loop was dipped into the melt and a small (≃100 mg) sample of melt was drawn and quenched in water. Viscosity measurements were continued with decreasing temperature until crystallization occurred. Crystallization during the final cooling step for each sample resulted in erratic viscosity readings and was easily confirmed by inspection of loop samples obtained at those times.

After viscometry runs, the samples were poured from the crucible onto a steel plate. Chips of each sample were analysed by electron microprobe for composition and homogeneity and the results of these analyses are compared with the "weighed in" compositions in Table 1. Excellent agreement was found between the initial and final (analysed) compositions.

^{57}Fe Mössbauer spectra

The oxidation state and structural state of iron in quenched loop samples collected during the viscometry runs were determined using ^{57}Fe Mössbauer spectroscopy. The resonant absorption spectra were recorded at 298 K with a 25 mC ^{57}Co/Pd source on powdered samples mixed with plastic transoptic powder and pressed into thin discs. The absorber thickness was constrained to be ≃5 mg Fe/cm^2. Mirror image spectra were recorded over 512 channels. The data were analysed separately and the results are the average values obtained from the left and right sides. The spectral data were deconvoluted with a least-squares routine using Lorentzian lines and with area and width constraints as discussed by VIRGO and MYSEN (1985). It was not possible to fit the low-velocity component of the ferrous doublet of highly oxidized glasses (Table 2), despite the use of area constraints.

The calculated $Fe^{3+}/\Sigma Fe$ value and the hyperfine parameters, quadrupole splittings and isomer shifts for both ferrous and ferric iron are given in Table 2.

Quench glasses with compositions along the tectosilicate join are highly oxidized and $Fe^{3+}/\Sigma Fe$ is invariant as a function of Si/Fe^{3+}, within experimental error. For the tetrasilicate quench glasses, $Fe^{3+}/\Sigma Fe$ systematically decreases with increasing Fe^{3+}/Si. A similar effect is observed with increasing Al/Si in iron-bearing, alkali and alkaline-earth aluminosilicate glasses (MYSEN, 1988).

The values of ferric isomer shift for the alkali-silicate glasses are in the range of 0.23–0.29 mm/sec and are similar to the values found for oxidized Na_2O-SiO_2 glasses containing 5 wt.% Fe_2O_3 (VIRGO *et*

TABLE 1. Analyzed melt compositions.

	Electron microprobe analysis[1,2]				Stoichiometric		
Sample	Na_2O	Fe_2O_3[3]	SiO_2	total	Na_2O	Fe_2O_3	SiO_2
$Na_2Si_4O_9$-$Na_6Fe_4O_9$							
NS4-F5	21.21	5.31	73.48	(98.08)	21.82	5.11	73.07
NS4-F10	24.03	10.29	65.68	(98.26)	23.05	9.90	67.05
NS4-F20	25.93	18.93	55.14	(99.67)	25.30	18.63	56.07
NS4-F30	27.59	27.66	44.76	(100.23)	27.30	26.38	46.32
NS4-F40	29.05	34.27	36.68	(101.51)	29.10	33.31	37.60
NS4-F50	31.61	40.18	28.22	(101.75)	30.70	39.55	29.76
SiO_2-$NaFeO_2$							
SFN6	5.96	15.54	78.50	(97.45)	5.83	15.02	79.14
Fe-albite	10.89	27.78	61.34	(100.70)	10.65	27.43	61.93
Acmite	14.10	35.78	50.12	(100.51)	13.41	34.56	52.02

[1] Wavelength dispersive analyses using a JEOL JSM-35 instrument and Krisel control system at: 15 kV accelerating voltage, 60 nA beam current on carbon, 30 sec maximum count times and continuously moving the sample under a 10 x 10 micron rastered beam. Synthetic glass standards were used. Maximum relative uncertainties at 3 s.d. are: 2.4% (Na), 2.0% (Fe) and 1.7% (Si). Oxygen by stoichiometry.
[2] Analyses normalized to 100% for comparison with stoichiometry.
[3] All iron recalculated as Fe_2O_3.

TABLE 2. ^{57}Fe Mössbauer parameters at 298K for glasses[1] along the SiO_2-$NaFeO_2$ and $Na_2Si_4O_9$-$Na_6Fe_4O_9$ joins[1].

Sample	ferric/total iron	Fe^{3+}		Fe^{2+}	
		I.S.[2]	Q.S.[3]	I.S.	Q.S.
NS4F5	0.82	0.28	0.83	0.89	1.96
NS4F10	0.89	0.29	0.82	0.87	2.21
NS4F20	0.95	0.25	0.86	1.02	2.04
NS4F30	1.0	0.24	0.86	(4)	(4)
NS4F40	0.98	0.22	0.86	(5)	(5)
NS4F50	1.0	0.21	0.85	(4)	(4)
SFN6	0.92	0.23	0.90	0.83	1.83
Fe-albite	0.94	0.24	0.86	(5)	(5)
Acmite	0.95	0.23	0.90	0.87	1.83

[1] all melts equilibrated with air.
[2] isomer shift (mm/sec).
[3] quadrupole splitting (mm/sec).
[4] 2 line fit, see text.
[5] 3 line fit, see text.

al., 1983). The isomer shift values for Fe^{2+} are >0.83 mm/sec and are also similar to those found for oxidized alkali and alkaline-earth aluminosilicates (VIRGO *et al.*, 1983; VIRGO and MYSEN, 1985). The isomer shift values for ferric iron are consistent with tetrahedrally-coordinated iron (see VIRGO and MYSEN, 1985, for a detailed discussion and review).

RESULTS

The Na_2O-FeO-Fe_2O_3-SiO_2 system

The viscosity data are presented in Table 3 and plotted as function of reciprocal absolute temperature in Fig. 2 ($Na_2Si_4O_9$-$Na_6Fe_4O_9$) and Fig. 3 (SiO_2-$NaFeO_2$). The viscosities of melts on the $Na_2Si_4O_9$-$Na_6Fe_4O_9$ join exhibit a trend of decreasing viscosity with decreasing $Na_2Si_4O_9$ content (Fig. 2). Similarly, the viscosities of melts on the SiO_2-$NaFeO_2$ join decrease with decreasing silicate content.

The temperature-dependence of the viscosities of some melts investigated in the Na_2O-FeO-Fe_2O_3-SiO_2 system may

TABLE 3. Viscometry data.

$Na_2Si_4O_9$-$Na_6Fe_4O_9$

NS4F5		NS4F10		NS4F20		NS4F30		NS4F40		NS4F50	
T	log η	T	log η	T	log η	T	log η	T	log η	T	log η
1401	1.94	1417	1.73	1402	1.20	1392	0.74	1408	0.33	1384	0.07
1346	2.11	1358	1.80	1351	1.33	1353	0.84	1352	0.47	1332	0.20
1287	2.31	1301	1.98	1292	1.47	1294	1.02	1295	0.67	1278	0.37
1231	2.50	1242	2.19	1233	1.68	1236	1.22	1239	0.81	1226	0.52
1179	2.70	1188	2.37	1178	1.87	1182	1.40	1186	0.98	1172	0.71
1127	2.94	1135	2.58	1128	2.06	1126	1.62	1124	1.21	1119	0.90
1073	3.20	1081	2.83	1074	2.30	1089	1.76	1068	1.41	1067	1.11
1018	3.52	1027	3.19	1024	2.52	1019	2.12	1011	1.71	1012	1.30
961	3.83	975	3.37	970	2.80	962	2.36	957	1.97	956	1.65
-	-	922	3.71	914	3.12	906	2.67	905	2.27	-	-
-	-	860	4.14	879	3.34	844	3.04	851	2.61	-	-
-	-	809	4.59	-	-	-	-	-	-	-	-

SiO_2-$NaFeO_2$

SFN6		Fe-albite		Acmite	
1426	3.51	1447	2.12	1408	1.41
1372	3.75	1403	2.28	1362	1.54
1319	4.01	1353	2.46	1312	1.73
1267	4.33	1301	2.69	1260	1.94
-	-	1250	2.92	-	-
-	-	1202	3.16	-	-
-	-	1149	3.44	-	-
-	-	1101	3.77	-	-
-	-	1053	4.14	-	-

Temperatures are ± 2°C, viscosities are ± 6% or 0.05 poise, whichever is larger.

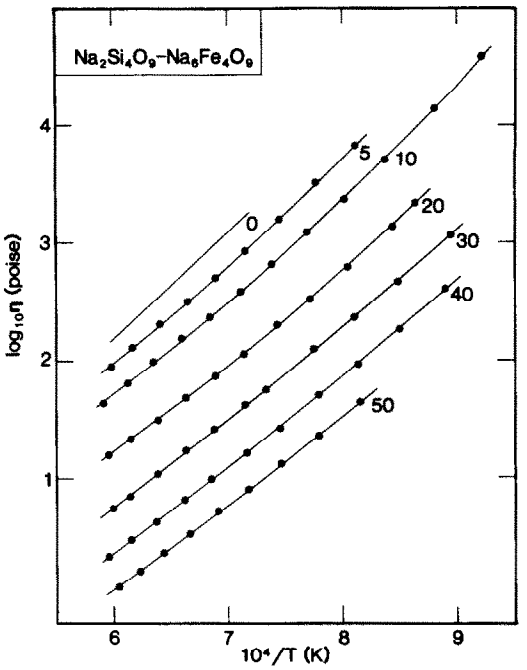

FIG. 2. Viscosity temperature relationships on the $Na_2Si_4O_9$-$Na_6Fe_4O_9$ join.

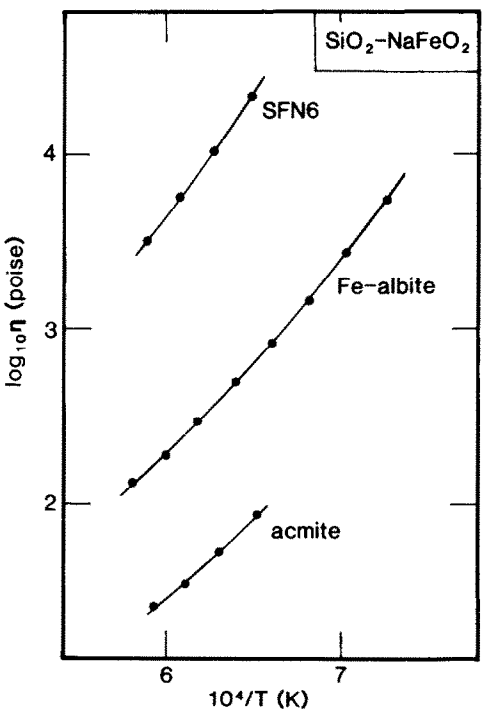

FIG. 3. Viscosity temperature relationships on the SiO_2-$NaFeO_2$ join.

be described within error as linear functions of reciprocal temperature and thus may be fitted to an equation of the form:

$$\log_{10} n = \log_{10} n_0 + Ea/2.303RT \qquad (1)$$

where n_0 and Ea are constants, termed the pre-exponential factor and the activation energy, respectively, R is the gas constant and T is the absolute temperature. The "Arrhenius" equations derived from these linear reciprocal temperature fits are presented in Table 4.

More generally, however, the observed viscosity-temperature relationships of Figs. 2 and 3 illustrate a non-linear (non-Arrhenian) dependence of viscosity on reciprocal absolute temperature. Several investigators have observed this behavior for silicate melts (*e.g.*, RICHET, 1984). In this study, data were obtainable over the largest temperature ranges for Fe-albite and NS4F10 and these melts best illustrate the non-linearity for the SiO_2-$NaFeO_2$ and $Na_2Si_4O_9$-$Na_6Fe_4O_9$ joins, respectively.

The non-linearity of the viscosity-temperature relationship may be incorporated into Eqn. (1) by the addition of a third adjustable parameter, denoted T_0, and termed the fictive temperature:

$$\log_{10} n = \log_{10} n_0 + Et/2.303R(T - T_0). \qquad (2)$$

The results of fits to this equation, termed the TVF (Tammann-Vogel-Fulcher) equation, are also presented in Table 4. The value of the slope parameters (Ea and Et) obtained from these two equations indicate that the viscosity-temperature relationships of melts on both the tetrasilicate and tectosilicate joins are not strong functions of composition.

Existing data for the Na_2O-Al_2O_3-SiO_2, Na_2O-B_2O_3-SiO_2 and Na_2O-Ga_2O_3-SiO_2 systems

The viscosity-temperature relationships of melts on the $Na_2Si_4O_9$-$Na_6Fe_4O_9$ and SiO_2-$NaFeO_2$ joins (Figs. 2, 3) are compared with the viscosity-temperature relationships for aluminum-bearing melts of equivalent stoichiometry (*i.e.*, compositionally related by the $Fe^{3+}Al_{-1}$ exchange operator) in the system Na_2O-Al_2O_3-SiO_2 in Figs. 4 and 5 (inset) ($Na_2Si_4O_9$-$Na_6Al_4O_9$ data from DINGWELL, unpublished; SiO_2-$NaAlO_2$ data from RIEBLING, 1966). The viscosities of melts on the $Na_2Si_4O_9$-$Na_6Al_4O_9$ and SiO_2-$NaAlO_2$ joins are considerably higher than the viscosities of melts on the $Na_2Si_4O_9$-$Na_6Fe_4O_9$ and SiO_2-$NaFeO_2$ joins, respectively. The viscosity-composition relationships are, however, qualitatively similar for the SiO_2-$NaFeO_2$ and SiO_2-$NaAlO_2$ joins

TABLE 4. Arrhenius and TVF coefficients.

	Arrhenius		Tammann-Vogel-Fulcher		
Sample	Ea[1]	$-\log_{10}n_0$	Et[1]	$-\log_{10}n_0$	T_0
NS4F5	40.8	3.41	23.9	1.95	333
NS4F10	39.8	3.53	20.4	1.71	373
NS4F20$_2$	36.3	3.58	22.1	2.32	301
NS4F30[c]	35.9	3.98	-	-	-
NS4F40	35.2	4.27	21.2	3.02	301
NS4F50	33.7	4.39	21.4	3.34	287
SFN6[2]	61.9	4.41	-	-	-
Fe-albite	52.7	4.61	27.0	2.46	427
Acmite	42.6	4.14	-	-	-

[1] Ea and Et in units of kcal/mole
[2] Arrhenius behavior within error

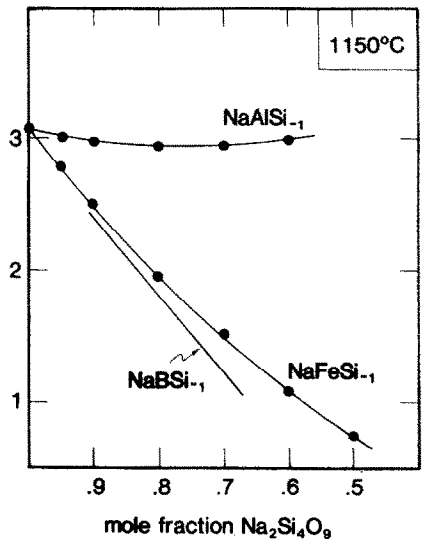

FIG. 4. Comparison of viscosities of melts on the $Na_2Si_4O_9$-$Na_6Fe_4O_9$ and $Na_2Si_4O_9$-$Na_6Al_4O_9$ joins at 1150°C. Boron-bearing melt data from TAIT *et al.* (1984). Aluminum-bearing melt data from DINGWELL (unpublished).

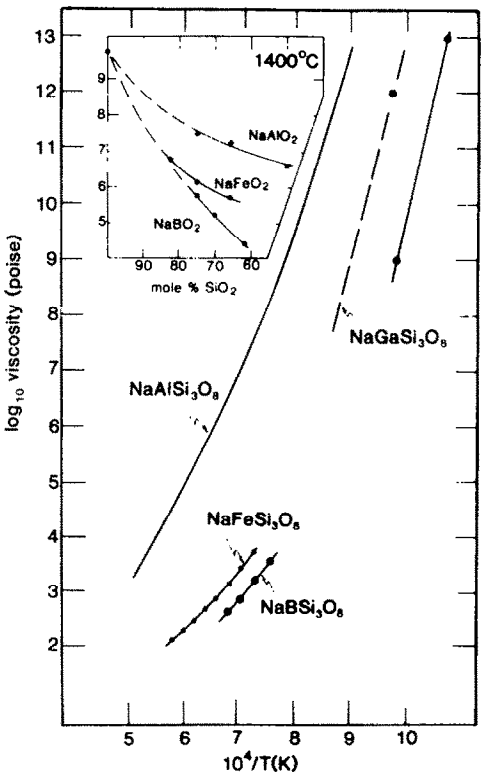

FIG. 5. Comparison of the viscosity temperature relationships of melts of $NaAlSi_3O_8$, $NaFeSi_3O_8$, $NaBSi_3O_8$ and $NaGaSi_3O_8$. (inset: comparison of the viscosities of melts on the SiO_2-$NaAlO_2$, SiO_2-$NaFeO_2$ and SiO_2-$NaBO_2$ joins at 1400°C.) Data from DAY and RINDONE (1962) and RIEBLING (1966), this work, TAIT *et al.* (1984) and LAPP and SHELBY (1984).

but quite different for the $Na_2Si_4O_9$-$Na_6Fe_4O_9$ and $Na_2Si_4O_9$-$Na_6Al_4O_9$ joins.

TAIT *et al.* (1984) have determined the viscosity-temperature relationships of sixteen melts in the Na_2O-B_2O_3-SiO_2 system in air, over the temperature range of 950–1500°C. The composition range of their investigation includes portions of the $Na_2Si_4O_9$-$Na_6B_4O_4$ (mole fraction $Na_6B_4O_9$ = 0.13 to 0.38) and SiO_2-$NaBO_2$ (mole fraction $NaBO_2$ = 0.20 to 0.55) compositional joins. TAIT *et al.* (1984) fitted their isothermal viscosity-composition data to a series of cubic polynomials at four temperatures (1050, 1100, 1150 and 1200°C). The resulting residuals are <0.03 $\log_{10}$ units of viscosity. The viscosity-temperature relationships of the borosilicate melts represented in Figs. 4 and 5 (inset) are derived from Eqn. 5 of TAIT *et al.* (1984). The viscosity-temperature relationships of sodium borosilicate melts in Figs. 4 and 5 (inset) are restricted to the ranges of composition and temperature of the TAIT *et al.* (1984) study, and are thus interpolations of the data.

The principal observation from Figs. 4 and 5 (inset) is that viscosities for Na_2O-Fe_2O_3-SiO_2 and Na_2O-B_2O_3-SiO_2 melts are similar. The viscosity of melts along the $Na_2Si_4O_9$-$Na_6B_4O_9$ and SiO_2-$NaBO_2$ joins decrease smoothly with decreasing silicate content. The viscosities of the boron-bearing melts are systematically lower than the equivalent iron-bearing melts over the entire range of comparison. The similarity of the bulk viscosities and the viscosity-temperature relationships of melts in the Na_2O-Fe_2O_3-SiO_2 and Na_2O-B_2O_3-SiO_2 systems contrasts with the much higher bulk viscosities and larger temperature dependencies of melts in the Na_2O-Al_2O_3-SiO_2 system.

SHELBY and coworkers (PIGUET and SHELBY, 1985; PIGUET *et al.*, 1985; LAPP and SHELBY, 1986) have investigated the (glass) transformation-range viscosity of several compositions in alkali galliosilicate systems. LAPP and SHELBY (1986) report viscosity data for several melts/glasses in the Na_2O-Ga_2O_3-SiO_2 system. The data were obtained using a beam-bending viscometer in the temperature range of 400 to 800°C. The data, although not tabulated, are presented in the form of isokom (iso-viscosity) curves of temperature *versus* composition at constant SiO_2 or Na_2O content. The 10^{12} poise (10^{11} Pa-s) isokom passes through $NaGaSi_3O_8$ (Ga-albite) composition at 750°C (as read from Fig. 9; LAPP and SHELBY, 1986); this data has been plotted in Fig. 5. The viscosity-temperature relationship is not reported for $NaGaSi_3O_8$ but is reported (from 670–730°C) for another composition on the SiO_2-$NaGaO_2$ join ($0.6SiO_2$-$0.4NaGaO_2$, Fig. 8, LAPP and SHELBY, 1986). This viscosity-temperature relationship is shown in Fig. 5 and has been used as a first approximation to the slope of the viscosity-temperature relationship of $NaGaSi_3O_8$ melt (dashed line, Fig. 5). The justification for this approximation is that the SiO_2-$NaFeO_2$, SiO_2-$NaAlO_2$ and SiO_2-$NaBO_2$ joins show a weak composition-dependence of the slope of the viscosity-temperature relationship in the range of mole fraction SiO_2 = 0.5 to 0.75.

Figure 5 provides a comparison of the viscosity-temperature relationships of $NaAlSi_3O_8$, $NaFeSi_3O_8$, $NaBSi_3O_8$ and $NaGaSi_3O_8$. The viscosity-temperature of $NaAlSi_3O_8$ has been extended to lower temperatures in Fig. 5 using the low temperature data of TAYLOR and RINDONE (1970). The important point to be noted from Fig. 5 is that the viscosity of $NaGaSi_3O_8$ is significantly lower than that of $NaAlSi_3O_8$ (approximately 3.75 $\log_{10}$ units). Additionally, the measured viscosity-temperature relationship of $NaAlSi_3O_8$ is subparallel to that which was estimated above for $NaGaSi_3O_8$. We do not advise a quantitative extrapolation of the estimated $NaGaSi_3O_8$ viscosity-temperature relationship to higher temperature, but we consider it likely, based on the data in Fig. 5, that the high temperature viscosity of $NaGaSi_3O_8$ is similar to those of $NaBSi_3O_8$ and $NaFeSi_3O_8$ melts.

Thus, it is clear from the available data that the viscosities of melts in the Na_2O-Fe_2O_3-SiO_2, Na_2O-B_2O_3-SiO_2 and Na_2O-Ga_2O_3-SiO_2 systems are significantly lower than the viscosities of equivalent melts in the Na_2O-Al_2O_3-SiO_2 system. Moreover, all the available data on the viscosity-temperature relationships of melts in these systems indicate that the *relative* bulk viscosities of melts in these four systems are not sensitive functions of temperature. On the basis of the premise that melt structure determines melt viscosity, and on the evidence (reviewed below) for the coordination of Al^{3+}, Fe^{3+}, B^{3+} and Ga^{3+} in these melts; we now propose to rationalize the relative bulk viscosities of melts in the systems Na_2O-Al_2O_3-SiO_2, Na_2O-Fe_2O_3-SiO_2, Na_2O-B_2O_3-SiO_2 and Na_2O-Ga_2O_3-SiO_2 in terms of the structural effects of substituting each of these trivalent cations for Si in these melts.

DISCUSSION

Discussion of the significance of the temperature- and composition-dependence of viscosities of any iron-bearing melts is made difficult by changes in redox state as a function of temperature and bulk composition. The relationship between the redox state and viscosities of melts in the Na_2O-FeO-Fe_2O_3-SiO_2 system has recently been investigated in a companion paper (DINGWELL and VIRGO, 1987). Figures 2 and 3 of DINGWELL and VIRGO (1987) illustrate that viscosities of melts in this study containing $\approx$95% ferric iron are lower than the viscosities one would estimate for the fully oxidized (100% ferric iron) equivalent melts by a $\log_{10}$ factor of $\approx$0.05. This difference between viscosities of melts equilibrated in air and their fully oxidized equivalents is insignificant in the discussion and comparisons to follow where the iron-bearing melts of this study are approximated to represent fully oxidized melts.

Similarly, the temperature-dependence of these melts is complicated by the temperature-dependence of redox equilibria. These melts will become more oxidized with decreasing temperature with the result that the temperature-dependence of their viscosities will be larger than that for an isochemical (constant ferric/ferrous ratio) melt. No further quantitative discussion of the temperature-dependence of viscosities of these iron-bearing melts is attempted at this time.

Coordination of Al^{3+}, Fe^{3+}, B^{3+} and Ga^{3+}

The short-range structure of melts in the Na_2O-Al_2O_3-SiO_2 system has been studied extensively. The structural role of aluminum in subaluminous (mol% Na = mol% Al) and peralkaline (mol% Na > mol% Al) melts in the Na_2O-Al_2O_3-SiO_2 system is generally agreed to be that of a tetrahedrally-coordinated trivalent cation which may be classified as a

network-former. The charge deficiency of a trivalent cation coordinating four bridging oxygens is compensated by a sodium cation near the aluminate tetrahedron which stabilizes the tetrahedral coordination of aluminum and the sharing of bridging oxygens between aluminate and silicate tetrahedra. The sharing of oxygens between tetrahedral cations is the essential requirement for polymerization or network formation in molten silicates so the sodium cation may be termed a network stabilizer.

Evidence for this structure model of melts in the portion of the Na_2O-Al_2O_3-SiO_2 system of concern to us here (that portion bounded by the tectosilicate and tetrasilicate joins) comes from a variety of structural probes, including Raman spectroscopy (SHARMA *et al.*, 1978; MYSEN *et al.*, 1981,1985b; MCMILLAN *et al.*, 1982; SEIFERT *et al.*, 1982; MATSON and SHARMA, 1985; MATSON *et al.*, 1986), X-ray fluorescence spectra (DAY and RINDONE, 1962), X-ray radial distribution functions (XRDF) (TAYLOR and BROWN, 1979a,b) and luminescence and X-ray photoelectron spectroscopy (ONORATO *et al.*, 1986). Additionally, indirect evidence for fully polymerized melts and glasses along the SiO_2-$NaAlO_2$ join (and therefore complete tetrahedral coordination of Al) is provided by discontinuities in composition-dependence of several physical properties at Na/Al = 1 (*e.g.*, viscosity, RIEBLING, 1966; density and index of refraction, DAY and RINDONE, 1962; He diffusivity, SHELBY and EAGAN, 1976 and the redox ratio Fe^{2+}/Fe^{3+}, DICKENSON and HESS, 1981,1986a).

The coordination of ferric iron in silicate melts has also received considerable attention in recent years. Compositions in the Na_2O-FeO-Fe_2O_3-SiO_2 system have been investigated by several methods, including ^{57}Fe Mössbauer spectroscopy (DANCKWERTH and VIRGO, 1982; FLEET *et al.*, 1984; DINGWELL and VIRGO, 1987), EXAFS (BROWN *et al.*, 1979), XRDF (HENDERSON *et al.*, 1984), optical absorption and luminescence spectroscopy (FOX *et al.*, 1982), and ESCA (GOLDMAN, 1986). The consensus of the above workers is that ferric iron is tetrahedrally coordinated in the relatively oxidized melts in the Na_2O-FeO-Fe_2O_3-SiO_2 system that result from equilibration with air.

Glasses in the Na_2O-B_2O_3-SiO_2 system have been investigated using B^{11} NMR spectroscopy (YUN and BRAY, 1978). Several B-bearing structural species, involving both trigonal and tetrahedral coordination of B^{3+}, have been identified. YUN and BRAY suggest that the B^{11} NMR spectra of glasses on the SiO_2-$NaBO_2$ join are consistent with tetrahedral coordination of B^{3+} (as $BSi_4O_{10}^-$ units) in the silicate network, from pure SiO_2 to $SiO_2/B_2O_3 = 8$ (or mole% $NaBO_2 = 20\%$ on the SiO_2-$NaBO_2$ join). Beyond this $NaBO_2$ content, the structure of the glasses contains an increasing fraction of B^{3+} which is excluded from the silicate network to form borate structural units involving tetrahedral and/or trigonal coordination of B^{3+} (*e.g.*, ring-type metaborate, diborate; YUN and BRAY, 1978). OESTRIKE *et al.* (1986) have provided additional high resolution NMR evidence for the both tetrahedral and trigonal coordination of B^{3+} in glasses on the reedmergnerite-albite join ($NaBSi_3O_8$-$NaAlSi_3O_8$). The proportion of trigonally coordinated B^{3+} decreases with increasing reedmergnerite content, and the proportion of B^{3+} in trigonal coordination in reedmergnerite glass (25 mole% $NaBO_2$) is given by OESTRIKE *et al.* (1986) as 29%.

The coordination of gallium in glasses in the Na_2O-Ga_2O_3-SiO_2 system has been investigated by Raman spectroscopy (VIRGO *et al.*, 1979; HENDERSON *et al.*, 1985; MATSON and SHARMA, 1985) and X-ray absorption spectroscopy (EXANES and EXAFS; FLEET *et al.*, 1984). These structural studies are in agreement in concluding that Ga^{3+} is tetrahedrally-coordinated in melts in the Na_2O-Ga_2O_3-SiO_2 system. This structural inference is supported by the binary nature of Ga-Al interdiffusion reported by KUSHIRO (1983) and (similar to the case for aluminum) by discontinuities in the temperature-dependence of physical properties such as viscosity (LAPP and SHELBY, 1986), He diffusivity (SHELBY, 1981) and the Fe^{2+}/Fe^{3+} ratio (DICKENSON and HESS, 1986b) at the Na/Ga = 1 compositional join which suggest that these (Na/Ga = 1) melts are fully polymerized.

Comparison of structure and properties of "tectosilicate" melts

If melts along the SiO_2-$Na(X)O_2$ joins (X = Al, Fe, B, Ga) exhibited tetrahedral coordination of all trivalent cations, then each of these "tectosilicate" compositions would yield structures that are equivalent in the sense that all are fully polymerized tectosilicate frameworks. As reviewed above, completely tetrahedral coordination is evidenced by spectroscopic studies of aluminosilicate, ferrosilicate and galliosilicate glasses, whereas borosilicate glasses are depolymerized by the existence of trigonally-coordinated B^{3+}. Non-tetrahedral coordination of some B^{3+} is also supported by the observation that melts along the SiO_2-$NaBO_2$ join do not represent viscosity maxima along constant SiO_2 joins (TAIT *et al.*, 1984) as is the case in the aluminosilicate and galliosilicate systems (RIEBLING, 1966; LAPP and SHELBY, 1986). Thus, the lower bulk viscosities of the borosilicate melts may be readily attributed to the trigonal coordination of some B^{3+} and the resulting depolymerized state of these melts. The contrast between the bulk viscosities of the aluminosilicate melts *versus* the ferrosilicate and galliosilicate melts requires a different structural explanation.

Cationic electronegativities

The relative viscosities of melts on the SiO_2-$NaFeO_2$, SiO_2-$NaAlO_2$, SiO_2-$NaBO_2$ (and possibly SiO_2-$NaGaO_2$) joins are inversely related to the electronegativities of the trivalent cations. The electronegativity of a cation may be viewed as the electron affinity of an ion during bond formation and the difference in cationic and anionic electronegativities is a measure of the ionicity (or percent ionic character) of the chemical bond. Although quantitative application of published cationic electronegativity scales (derived for the gaseous state) to actual cation-oxygen bond strengths in condensed silicates is not recommended, some qualitative observations may be made. Typical cationic electronegativities of Ga, Fe and B are 1.6, 1.9 and 2.0, respectively (PAULING, 1960). All are higher than Al (1.45) and thus Fe, B and Ga can be expected to compete with Si for the bonding electrons of bridging oxygens more effectively than Al. Such competition may result in increased tetrahedral bond angle distortion and the resulting creation of more than one structural unit of intermediate range. The importance of electronegativities in influencing the Raman spectra of sodium alumino- and gal-

liosilicate melts has been noted previously by MATSON and SHARMA (1985).

Viscosity data from URBAIN *et al.* (1982) for alkali and alkaline earth aluminosilicate melts, presented in Fig. 6 reveal further systematics involving cationic electronegativities and melt viscosities. Figure 6 illustrates that melts along the tectosilicate joins, SiO_2-XAl_2O_4 (where X = Ba, Sr, Ca, Mg) exhibit an inverse correlation between viscosity and the electronegativity of the (in this case) network-stabilizing, alkaline earth cation [Pauling electronegativities are: Ba (0.9), Sr (1.0), Ca (1.0), Mg (1.2)]. The data available for these melts (Fig. 6) indicate that the order of decreasing viscosity does not depend on either temperature or SiO_2 content.

Figure 6 illustrates the same general behavior for alkali-bearing melts. The sparse data for melts on the SiO_2-$XAlO_2$ joins (where X = K, Na, Li; $LiAlSi_3O_8$ data from SHELBY, 1978) are consistent with an inverse relationship between melt viscosity and cation electronegativity [Pauling electronegativities are: K (0.8), Na (0.9), Li (1.0)].

One further point of comparison between tectosilicate melt viscosities is that the viscosities of the alkaline earth aluminosilicate melts are lower than those of the alkali aluminosilicate melts. The lower viscosities of the alkaline earth melts would then indicate that our electronegativity-viscosity relationship cannot be applied directly across chemical groups. We will return to the comparison of alkali and alkaline earth aluminosilicate melt viscosities in a later section on calorimetric data.

T-O-T bond angle variation

Several studies have proposed that the $NaAlSi_{-1}$ substitution results in a decrease in average T-O-T bond angle of melts along the SiO_2-$NaAlO_2$ join and the estimates of relative change in T-O-T bond angle from SiO_2 to $NaAlSiO_4$ (*i.e.* 50% completion of the $NaAlSi_{-1}$ substitution) from Raman spectra (SEIFERT *et al.*, 1982) and from XRD data (KONNERT and KARLE, 1973; TAYLOR and BROWN, 1979b; DEJONG and BROWN, 1980) are (comparable at) 4.6% and 5.8%, respectively. Estimation of the average T-O-T bond angle in vitreous SiO_2 and $NaFeSi_3O_8$ by HENDERSON *et al.* (1984) yields a change in T-O-T bond angle, with only 25% completion of the $NaFeSi_{-1}$ exchange (from silica to Fe-albite), of 7.3%. Thus, comparison of the decreases of the average T-O-T bond angles for the SiO_2-$NaAlO_2$ and SiO_2-$NaFeO_2$ joins is consistent with the suggestion that the effect of the $NaFeSi_{-1}$ substitution is much larger (7.3% at 25% substitution) than the effect of the $NaAlSi_{-1}$ substitution (≈4–6% at 50% substitution).

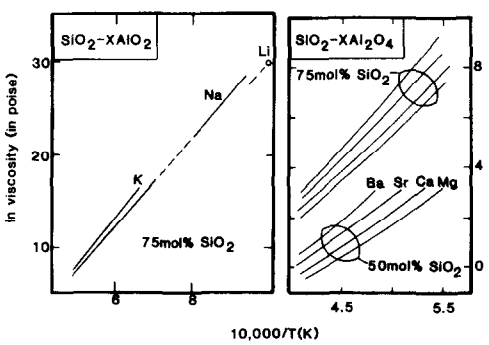

FIG. 6. Comparison of the viscosity-temperature relationships of both alkaline earth and alkali aluminosilicate melts. Data from SHELBY (1978); URBAIN *et al.* (1982).

VIRGO *et al.* (1979) and HENDERSON *et al.* (1985) have discussed their Raman spectral data of glasses along the SiO_2-$NaGaO_2$ join in terms of potential intermediate range structures. It is evident from Fig. 33 of VIRGO *et al.* (1979) that the frequency shift for the Si-O (bridging) stretching mode (at approx. 1070 cm^{-1} in pure SiO_2) as a function of composition is larger for glasses on the SiO_2-$NaFeO_2$ and SiO_2-$NaGaO_2$ joins. This observation is consistent with the suggestion that the $NaFeSi_{-1}$ and $NaGaSi_{-1}$ substitutions have a larger effect than the $NaAlSi_{-1}$ substitution on the tectosilicate structure.

Thus, the evidence for the structural effects of both the $NaGaSi_{-1}$ and the $NaFeSi_{-1}$ substitutions may be interpreted similarly in that incorporation of Fe-tetrahedra or Ga-tetrahedra into SiO_2 melt results in perturbation of the network structure as evidenced by the large decrease observed in the average T-O-T bond angle.

Related information for a hypothetical tectosilicate structure of melts on the SiO_2-$NaBO_2$ join comes from the *ab initio* molecular orbital calculations of GEISINGER *et al.* (1985). NAVROTSKY *et al.* (1985) present the variation of calculated potential energy as a function of T-O-T bond angle for B-O-B, B-O-Si, Al-O-Al, Al-O-Si and Si-O-Si derived from calculations for groups of the general formula $H_6X_2O_7^{n-}$ (where X = Si, Al, B and n = 2–4). The potential energy curves indicate that for the aluminosilicate group, the Si-O-Al, Al-O-Al and Si-O-Si bonds have relatively broad minima as a function of T-O-T bond angle and the minima are in the T-O-T bond angle range of 135 to 150°. In contrast, the borosilicate groups exhibit relatively narrow potential energy minima for the B-O-B and B-O-Si bonds that occur at lower values of the T-O-T bond angle (125 to 133°). NAVROTSKY *et al.* (1985) suggest that the lower value of T-O-T bond angle and the relative "inflexibility" of this angle for bonds involving B^{3+} rather than Al^{3+} poses a potential energy barrier to the substitution of borate for silicate tetrahedra in borosilicate melts.

Enthalpy of solution

The heat of reaction obtained from solution of glasses (LN_2—quenched from liquids at 1893 K) of the general formula $X^{n+}_{1/n}AlO_2$-SiO_2 (where M = K, Na, Ba, Sr, Ca, Mg) into $2PbO \cdot B_2O_3$ at 973 K are provided by ROY and NAVROTSKY (1984, Fig. 2). The relative values of heats of solution (H_{sol}) provide information on the relative strengths of bonds broken during the dissolution process. The values of H_{sol} become more exothermic with increasing cation electronegativity (from K to Mg) and, as noted by NAVROTSKY *et al.* (1985), the decrease in average bond strength, inferred from more exothermic values of H_{sol}, correlates with decreasing viscosities for these compositions.

Figure 7 is a comparison of viscosity (1400°C) and H_{sol} ($2PbO \cdot B_2O_3$, 973 K) for aluminosilicate melts of the general formula $X^{n+}_{1/n}AlSi_3O_8$ (where X = K, Na, Ba, Sr, Ca, Mg). A positive correlation exists between viscosity and H_{sol} for these melts containing 75 mol% SiO_2. In order to minimize the

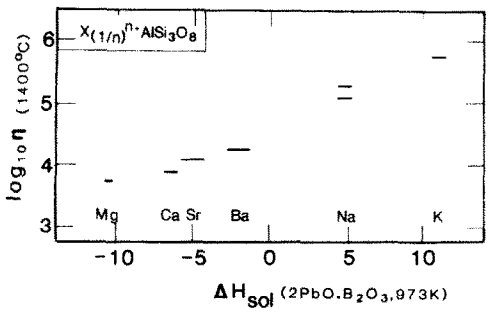

FIG. 7. Viscosities of melts of the general composition $X_{1/n}^{n+}AlSi_3O_8$ (where X = Mg, Ca, Sr, Ba, Na, K) at 1400°C plotted *versus* the enthalpy of solution of equivalent glasses obtained in molten $2PbO \cdot B_2O_3$ at 973 K. Viscosity data (in poise) from same sources as Fig. 6; enthalpy data (in kJ/mole based on 2 oxygens) from ROY and NAVROTSKY (1984). Discrepant albite (Na) data are from URBAIN *et al.* (1982) (higher value) and SCARFE and CRONIN (1986) (lower value); see text for discussion.

imprecision of viscosity data arising from comparison of different studies, all viscosity data were chosen from the study of URBAIN *et al.* (1982). The H_{sol} data are all from the study by ROY and NAVROTSKY (1984). A positive correlation between viscosity and H_{sol} is apparent. The data are insufficient to indicate whether the correlation is best described as one curve including both alkali- and alkaline earth-bearing melts or two subparallel curves, one each for alkali- and alkaline earth-bearing melts. High temperature viscosity data for $LiAlSi_3O_8$ are needed.

If the correlation of Fig. 7 is a single curve then the origin of the differences in viscosity between aluminosilicates on the tectosilicate joins may be attributed to differences in average bond strength. If there are, instead, two curves in Fig. 7, then average bond strength cannot entirely explain the relative melt viscosities, and aluminate tetrahedral ordering becomes a likely explanation for the difference between the two curves.

CONCLUSIONS

The examination of the available data on the structure and viscosity-temperature relationships of tectosilicate melts in the Na_2O-Al_2O_3-SiO_2, Na_2O-Fe_2O_3-SiO_2, Na_2O-B_2O_3-SiO_2 and Na_2O-Ga_2O_3-SiO_2 systems and comparison with equivalent data for both the alkaline earth and other alkali aluminosilicate systems, in combination with calorimetric and spectroscopic studies, leads to the following conclusions.

The viscosity-temperature relationships of these melts yield isothermal bulk viscosities that decrease in the order of aluminosilicate > ferrosilicate, (galliosilicate?) > borosilicate. The relative viscosities do not appear to be sensitive to the temperature of comparison.

The relative viscosities of tectosilicate melts are inversely correlated with the electronegativity of the substituted cation both for monovalent and divalent network-stabilizer cations *e.g.*, Li, Na, K and Mg, Ca, Sr, Ba) and for trivalent network-former cations. A substitution of the monovalent or divalent network-stabilizer cation or the trivalent network-former cation for a cation of greater electronegativity, yields a lower viscosity that results from weaker T-O-T bonds and a more distorted T-O-T bond angle population. The latter of these two effects (T-O-T bond angle distortion) may result, in the case of the network-former substitution, in a change in the ordering of trivalent network-formers. Thus the viscosity reduction with substitution to cations of higher electronegativity is explicable in terms of (1) weakened T-O bonds, and (2) T-O-T bond angle distortion (with possible ordering of tetrahedral cations). The estimate of average bond strength from solution calorimetry of silicate glasses may provide, in the future, evidence for a distinction between these two effects.

Acknowledgements—The authors wish to thank P. Hess, M. Fleet and an anonymous reviewer for their comments.

Editorial handling: P. C. Hess

REFERENCES

BAILEY D. K. and MACDONALD R. (1987) Dry peralkaline felsic liquids and carbon dioxide flux through the Kenya rift zone. In *Magmatic Processes: Physicochemical Principles* (ed. B. O. MYSEN). *Geochem. Soc., Special Publication* **1**, 91–105.

BOTTINGA Y. and WEILL D. F. (1972) The viscosity of magmatic silicate liquids: A model for calculation. *Amer. J. Sci.* **272**, 438–475.

BOWEN N. L., SCHAIRER J. F. and WILLEMS H. W. V. (1930) The ternary system: Na_2SiO_3-Fe_2O_3-SiO_2. *Amer. J. Sci.* **20**, 405–455.

BROWN G., KEEFER K. D. and FENN P. M. (1979) Extended X-ray absorption fine structure (EXAFS) study of iron-bearing silicate glasses: Iron coordination environment and oxidation state. (abstr.) *Geol. Soc. Amer. Abstr. Prog.* **11**, 373.

DANCKWERTH P. A. and VIRGO D. (1982) Structural state of iron in the system Na_2O-SiO_2-Fe-O. *Carnegie Inst. Wash. Yearb.* **81**, 340–342.

DAY D. E. and RINDONE G. E. (1962) Properties of soda aluminosilicate glasses. *J. Amer. Ceram. Soc.* **45**, 489–504, 579–581.

DEJONG B. H. W. S. and BROWN G. E. (1980) The polymerization of silicate and aluminate tetrahedra in glasses, melts and aqueous solutions—I. Electronic structure of $H_6Si_2O_7^-$, $H_6AlSi_2O_7^-$ and $H_6Al_2O_7^-$. *Geochim. Cosmochim. Acta* **44**, 491–511.

DICKENSON M. P. and HESS P. C. (1981) Redox equilibria and the structural role of iron in aluminosilicate melts. *Contrib. Mineral. Petrol.* **78**, 352–357.

DICKENSON M. P. and HESS P. C. (1986a) The structural role and homogeneous redox equilibria of iron in peraluminous, metaluminous and peralkaline silicate melts. *Contrib. Mineral. Petrol* **92**, 207–217.

DICKENSON M. P. and HESS P. C. (1986b) The structural role of Fe^{3+}, Ga^{3+}, Al^{3+} and homogeneous iron redox equilibria in K_2O-Al_2O_3-Ga_2O_3-SiO_2-Fe_2O_3-FeO melts. *J. Non-Cryst. Solids* **86**, 303–310.

DINGWELL D. B. (1986) Viscosity-temperature relationships in the system $Na_2Si_2O_5$-$Na_4Al_2O_5$. *Geochim. Cosmochim. Acta* **50**, 1261–1265.

DINGWELL D. B. and VIRGO D. (1987) The effect of oxidation state on the viscosity of melts in the system Na_2O-FeO-Fe_2O_3-SiO_2. *Geochim. Cosmochim. Acta* **51**, 195–205.

FISHER R. V. and SCHMINKE H.-U. (1984) *Pyroclastic Rocks*. Springer-Verlag, 472p.

FLEET M. E., HERZBERG C. T., HENDERSON G.S., CROZIER E. D., OSBORNE M. D. and SCARFE C. M. (1984) Coordination of Fe, Ga and Ge in high pressure glasses by Mössbauer, Raman and X-ray absorption spectroscopy, and geological implications. *Geochim. Cosmochim. Acta* **48**, 1455–1466.

FOX K. E., FURUKAWA T. and WHITE W. B. (1982) Transition metal ions in silicate melts. Part 2, Iron in sodium silicate glasses. *Phys. Chem. Glasses* **32**, 169–178.

GEISINGER K. L., GIBBS G. V. and NAVROTSKY A. (1985) A molecular orbital study of bond length and angle variations in framework structures. *Phys. Chem. Minerals* **11**, 266–283.

GOLDMAN D. S. (1986) Evaluation of the ratios of bridging to nonbridging oxygens in simple silicate glasses by electron spectroscopy for chemical analysis. *Phys. Chem. Glasses* **27**, 128–133.

HENDERSON G. S., FLEET M. S. and BANCROFT G. M. (1984) An X-ray scattering study of vitreous $KFeSi_3O_8$ and $NaFeSi_3O_8$ and reinvestigation of vitreous SiO_2 using quasi-crystalline modelling. *J. Non-Cryst. Solids* **68**, 333–349.

HENDERSON G. S., BANCROFT G. M., FLEET M. E. and ROGERS D. J. (1985) Raman spectra of gallium and germanium substituted silicate glasses: Variations in intermediate range order. *Amer. Mineral.* **70**, 946–960.

KONNERT J. H. and KARLE L. (1973) The computation of radial distribution functions for glassy materials. *Acta Crystal.* **29**, 702–710.

KUSHIRO I. (1983) Effect of pressure on the diffusivity of network-forming cations in melts of jadeitic composition. *Geochim. Cosmochim. Acta* **47**, 1415–1422.

LAPP J. C. and SHELBY J. E. (1986) Viscosity and thermal expansion of sodium and potassium galliosilicate glasses. *J. Amer. Ceram. Soc.* **69**, 126–131.

MATSON D. W. and SHARMA S. K. (1985) Structures of sodium alumino- and gallosilicate glasses and their germanium analogs. *Geochim. Cosmochim. Acta* **49**, 1913–1924.

MATSON D. W. and SHARMA S. K. and PHILPOTTS J. A. (1986) Raman spectra of some tectosilicates and of glasses along the orthoclase-anorthite and nepheline-anorthite joins. *Amer. Mineral.* **71**, 694–704.

MCMILLAN P. F., PIRIOU B. and NAVROTSKY A. (1982) A Raman spectroscopic study of glasses along the joins silica-calcium aluminate, silica-sodium aluminate and silica potassium aluminate. *Geochim. Cosmochim. Acta* **46**, 2021–2037.

MYSEN B. O. (1988) Relationships between structure, redox equilibria of iron and properties of magmatic liquids. In *Advances in Physical Chemistry* (eds. L. PERCHUK and I. KUSHIRO). In press.

MYSEN B. O., SEIFERT F. A. and VIRGO D. (1980) Structure and redox equilibria of iron-bearing silicate melts. *Amer. Mineral.* **65**, 867–884.

MYSEN B. O., VIRGO D. and KUSHIRO I. (1981) The structural role of aluminum in silicate melts—a Raman spectroscopic study at 1 atmosphere. *Amer. Mineral.* **66**, 678–701.

MYSEN B. O., VIRGO D., NEUMANN E.-R. and SEIFERT F. A. (1985a) Redox equilibria and the structural states of ferric and ferrous iron in melts in the system CaO-MgO-Al_2O_3-SiO_2-Fe-O: Relationships between redox equilibria, melt structure and liquidus phase equilibria. *Amer. Mineral.* **70**, 317–331.

MYSEN B. O., VIRGO D. and SEIFERT F. A. (1985b) Relationships between properties and structure of aluminosilicate melts. *Amer. Mineral.* **70**, 834–847.

NAVROTSKY A., GEISINGER K. L., MCMILLAN P. and GIBBS G. V. (1985) The tetrahedral framework in glasses and melts—inferences from molecular orbital calculations and implications for structure, thermodynamics, and physical properties. *Phys. Chem. Mineral.* **11**, 284–298.

OESTRIKE R., GEISINGER K., NAVROTSKY A. TURNER G. L. and KIRKPATRICK R. J. (1986) Structure and thermochemistry of glasses along the join $NaAlSi_3O_8$-$NaBSi_3O_8$: The effect of boron. *Geol. Soc. Amer. Abstr. Prog.* **18**, 709.

ONORATO P. I. K., ALEXANDER M. N., STRUCK C. W., TASKER G. W. and UHLMANN D.R. (1986) Bridging and nonbridging oxygen atoms in alkali aluminosilicate glasses. *J. Amer. Ceram. Soc.* **68**, C-148–150.

PAULING L. (1960) *The Nature of the Chemical Bond.* Cornell Univ. Press, Ithaca.

PIGUET J. L. and SHELBY J. E. (1985) Transformation-range behavior of Li_2O-$(Al,Ga)_2O_3$-SiO_2 glasses. *J. Amer. Ceram. Soc.* **68**, C-232–233.

PIGUET J. L., LAPP J. C. and SHELBY J. E. (1985) Transformation-range behavior of lithium galliosilicate glasses. *J. Amer. Ceram. Soc.* **68**, 326–329.

RICHET P. (1984) Viscosity and configurational entropy of silicate melts. *Geochim. Cosmochim. Acta* **48**, 471–483.

RIEBLING E. F. (1966) Structure of sodium aluminosilicate melts containing at least 50 mole% SiO_2 at 1500°C. *J. Chem. Phys.* **44**, 2857–2865.

ROY B. N. and NAVROTSKY A. (1984) Thermochemistry of charge-coupled substitutions in silicate glasses: The systems $M^{n+}_{1/n}AlO_2$-SiO_2 (M = Li, Na, K, Rb, Cs, Mg, Ca, Sr, Ba, Ph). *J. Amer. Ceram. Soc.* **67**, 606–610.

SCARFE C. M. and CRONIN D. J. (1986) Viscosity-temperature relationships of melts at 1-atm in the system diopside-albite. *Amer. Mineral.* **71**, 767–771.

SEIFERT F. A., MYSEN B. O. and VIRGO D. (1982) Three dimensional network structure of quenched melts (glass) in the systems SiO_2-$NaAlO_2$, SiO_2-$CaAl_2O_4$ and SiO_2-$MgAl_2O_4$. *Amer. Mineral.* **67**, 696–717.

SHARMA S. K., VIRGO D. and MYSEN B. O. (1978) Structure of melts along the join SiO_2-$NaAlSiO_4$ by Raman spectroscopy. *Carnegie Inst. Wash. Yearb.* **77**, 652–658.

SHELBY J. E. (1978) Viscosity and thermal expansion of lithium aluminosilicate glasses. *J. Appl. Phys.* **49**, 5885–5891.

SHELBY J. E. (1981) Helium migration in alkali galliosilicate glasses. *J. Non-Cryst. Solids*, **45**, 411–418.

SHELBY J. E. and EAGAN R. J. (1976) Helium migration in sodium aluminosilicate glasses. *J. Amer. Ceram. Soc.* **59**, 420–425.

TAIT J. C., MANDOLESI D. L. and RUMMENS H. E. C. (1984) Viscosity of melts in the sodium borosilicate system. *Phys. Chem. Glasses* **25**, 100–104.

TAYLOR M. and BROWN G. E. JR. (1979a) Structure of mineral glasses I. The feldspar glasses $NaAlSi_3O_8$, $KAlSi_3O_8$, $CaAl_2Si_2O_8$. *Geochim. Cosmochim. Acta* **43**, 61–74.

TAYLOR M. and BROWN G. E. JR. (1979b) Structure of mineral glasses II. The SiO_2-$NaAlSiO_4$ join. *Geochim. Cosmochim. Acta* **43**, 1467–1473.

TAYLOR I. D. and RINDONE G. E. (1970) Properties of aluminosilicate glasses: V. Low-temperature viscosities. *J. Amer. Ceram. Soc.* **53**, 692–695.

URBAIN G., BOTTINGA Y. and RICHET P. (1982) Viscosity of liquid silica, silicates and alumino-silicates. *Geochim. Cosmochim. Acta* **46**, 1061–1072.

VIRGO D. and MYSEN B. O. (1985) The structural state of iron in oxidized *versus* reduced glasses at 1 atm: A ^{57}Fe Mössbauer study. *Phys. Chem. Mineral.* **12**, 65–76.

VIRGO D., SEIFERT F. A. and MYSEN B. O. (1979) Three-dimensional network structure of glasses in the systems $CaAl_2O_4$-SiO_2, $NaAlO_2$-SiO_2, $NaFeO_2$-SiO_2 and $NaGaO_2$-SiO_2 at 1 atm. *Carnegie Inst. Wash. Yearb.* **78**, 506–511.

VIRGO D., MYSEN B. O. and DANCKWERTH P. A. (1983) Redox equilibria and the anionic structure of $Na_2O \cdot xSiO_2$-Fe-O melts: Effect of oxygen fugacity. *Carnegie Inst. Wash. Yearb.* **82**, 305–309.

WILLIAMS H. and MCBIRNEY A. R. (1979) *Volcanology.* Freeman, Cooper & Co., San Francisco, 397p.

YUN Y. H. and BRAY P. J. (1978) Nuclear Magnetic Resonance studies of glasses in the system Na_2O-B_2O_3-SiO_2. *J. Non-Cryst. Solids* **27**, 363–380.